Engineering Structures 126 (2016) 628–640

Contents lists available at ScienceDirect

Engineering Structures

journal homepage: www.elsevier.com/locate/engstruct

Dynamic characterization of the Eiffel tower

Silvia Castellaro [a,*], Luigi Perricone [b], Marco Bartolomei [c], Stefano Isani [c]

[a] Dipartimento di Fisica e Astronomia, Università di Bologna, viale C. B. Pichat 8, 40127 Bologna, Italy
[b] Studio di Geologia Rigo Perricone, Cividale del Friuli, Udine, Italy
[c] Consultant Engineer at Matildi + Partners, Bologna, Italy

ARTICLE INFO

Article history:
Received 24 February 2016
Revised 2 August 2016
Accepted 11 August 2016

Keywords:
Eiffel tower
Dynamic characterization

ABSTRACT

The Eiffel tower is the most visited monument in the world. Millions of visitors have taken millions of pictures of it over the last century but apparently a dynamic picture (that is a dynamic characterization) does not exist or is not publicly available. In this paper we show the amount of information that can be extracted from a few recordings of ambient tremor collected on the tower and on the surrounding subsoil with a single pocket seismometer in a few minutes, during a leisure visit. We also propose a numerical model for the tower, capable to fit the observed data. This is interesting because the mass and stiffness distribution of the tower is unique and does not follow any modern construction rule. The dynamic model of the tower would also be important if Paris were a high seismic hazard town, which is not. According to our model, the tower could withstand peak ground accelerations >100% larger than the values prescribed by current seismic hazard estimates. Regarding the wind, Eiffel could only study its effects from a static planar point of view, while the model allowed us to follow a 3D approach and to assess the expected displacements under different loads. Last, the dynamic model of the tower is also important to better design the future interventions and to monitor the ageing of the structure.

1. Introduction

One of us (L.P.) is used to spend his vacations in Paris and one day, while watching his pictures of the town, another one of us (S.C.) proposed him to take a different picture of the town most famous structure. This said, on November 13th 2015, these two of us left for Paris with a pocket seismometer in the backpack and decided to climb the Eiffel Tower to measure its dynamic behavior, since surprisingly nobody has done it before, at least to our knowledge based on bibliographic research. In the literature several studies about the tower shape [12,38] and its foundations [2] can be found, as well as studies on the tower behavior to wind [9,26,37]. According to the French newspaper Le Moniteur [21], a 2 year project to create a numerical model of the tower was going to be realized by the Société d'Exploitation de la Tour Eiffel but we have not found any further information on this.

Before leaving, we bet with two structural engineers (M.B. and S.I.), expert in steel structures, about what to expect from the measurements and they liked the idea of joining us in the subsequent numerical modelling.

Countries characterized by high seismic hazard are used to measure the dynamic response of buildings in order to tune their numerical models and better plan retrofitting actions and/or to quantify the results of a retrofit. However, according to the Global Seismic Hazard Map [14] and its revisions (SHARE Consortium, [39]), seismic hazard in Paris is low (the bedrock peak ground acceleration with 10% exceedance probability in 50 years is equal to 0.02–0.04 g only) and this is possibly one of the reasons why a dynamic characterization of the Eiffel tower is not apparently available. Nevertheless, the dynamic characterization of a structure is relevant not only to forecast or design its response to seismic actions but also, for example, to forecast or design its response to the wind actions. Gustave Eiffel studied the effect of wind on the tower but he could only approach this from a static point of view [10].

In addition to this, the dynamic characterization of the Eiffel tower is interesting because, beyond being the most visited paid monument in the world, the tower is very tall (more than 300 m) and light, which means that it is an unusual structure with a large stiffness and a small mass, whose behavior escapes any intuitive forecast.

In setting up a numerical model for the tower, another interesting fact arises: the non-structural masses of the tower changed over time. The original drawings of the Eiffel's engineering team are available [10]. In these drawings we could find the size and mass of every single structural and decorative element of the tower. However, it is easy to recognize that the non-structural

* Corresponding author.
E-mail address: silvia.castellaro@unibo.it (S. Castellaro).

http://dx.doi.org/10.1016/j.engstruct.2016.08.023
0141-0296/

masses are strongly different today, compared to 1889 and determining the distribution of the masses at present by fitting the numerical model with the experimental data is an interesting exercise.

2. Experimental survey

The Eiffel tower, one of the most iconic and popular buildings in the world, was designed by Gustave Eiffel and completed in 1889 for the World's Fair. From its construction to 1930, with its 324 m height, it was also the tallest building in the world. As anyone knows, it consists of a puddled iron lattice tower, divided into 3 levels, whose main geometrical features are summarized in Table 1. We note that these values are those declared by Eiffel himself in the original drawings [10] and that some of them have certainly changed over the years.

The foundations are 4 separate plinths for each leg (Table 1), which means – and which probably sounds unexpected to most engineers, 16 separate foundations. These are set at a depth of 7 m, where, according to the geological map (Fig. 1) and to the trenches dug during the tower construction, sands and gravels are present.

Before attempting any numerical modelling of the tower, we first characterized the dynamic behavior of the subsoil where it is founded and of the tower itself.

2.1. The subsoil

According to the official geological map [3] the area of the Champ de Mars in Paris is characterized by outcropping conglomerates (C in Fig. 1) and silts and sands (SS). The excavations, performed in 1887 for the construction of the tower foundations, actually revealed no conglomerates and silt and sand alternations in the first 20 m, with just a few meter thickness layer of chloritic limestone (Fig. 3 in Plate II, [10]).

In order to get some quantitative information about the local subsoil properties, we performed a type of geophysical prospection that can be acquired with a single instrument. This is based on the principle that the surface of the Earth is continuously excited by seismic waves produced by natural sources (e.g., atmospheric perturbations, wind, ocean waves etc.) and anthropic sources (traffic, human activities, etc.). These vibrations (called microtremor or ambient noise) are enough to make the subsoil vibrate at its resonance frequencies, exactly as a building vibrates at its modal frequencies under any excitation. In a single degree of freedom oscillator (SDOF, assumed as the basic model of simple structures), the resonance or modal frequencies of the oscillator are well known to be directly proportional to the stiffness k and inversely proportional to the mass m:

$$f_{SDOF} = \frac{1}{2\pi}\sqrt{\frac{k}{m}} \tag{1}$$

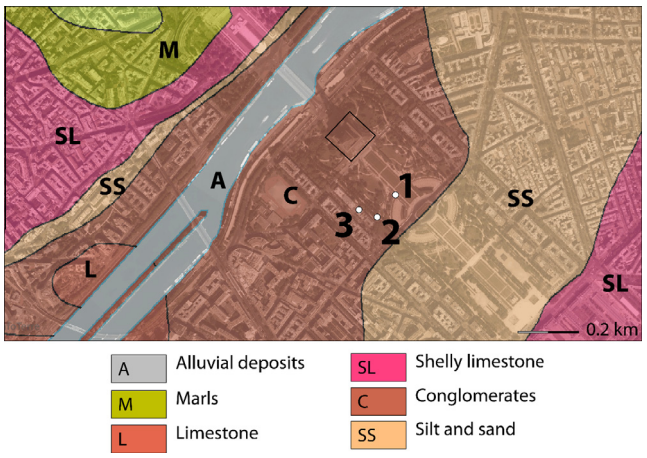

Fig. 1. Geological map redrawn from BRGM [3]. The perimeter of the Eiffel tower is marked by the black square. The numbers indicate the location of the H/V surveys.

Subsoils also are oscillators, whose stiffness μ is an elastic constant linked to the shear wave velocity V_S and density of the medium ρ, while the mass, being the subsoil interpreted as a laterally infinite medium, is described by the thickness H of the resonating layer.

$$f_{subsoil} = \frac{V_S}{4H}, \quad where\ V_S = \sqrt{\frac{\mu}{\rho}} \tag{2}$$

By comparing Eqs. (1) and (2) we note that the resonance frequency of a structure idealized as a SDOF oscillator and of an idealized subsoil are described by the same equation, with an extra 2 factor at the denominator of Eq. (2) (due to the phase reversal of seismic waves after the first reflection from a soft to a stiff layer, [40]). From Eq. (2) it is also clear that if we can measure the resonance frequency of a subsoil and we have an estimate of V_S in the same layer, then we can know its thickness and vice versa.

The microtremor spectra recorded at a site vary with the source producing them and have therefore seasonal and diurnal fluctuations. It has been shown, and is commonly accepted in the seismological literature, that the ratio between the horizontal and the vertical components (H/V) has an effective normalization power: it clears the source effect, thus revealing the path effect, that is the subsoil properties in terms of resonance frequency [4]. For the physical explanation we address to Fäh et al. [11], SESAME [28], Tuan et al. [35] and references therein.

We applied this subsoil exploration technique around the Eiffel tower (Fig. 1). Microtremor was recorded at 3 sites for 10 min at 512 samples per second with the 3-component tromometer Tromino® (MoHo s.r.l.). The recorded signal was divided into 30 s windows. The signal of each window was detrended, tapered with a Bartlett window, padded and FFT transformed. The average H/V

Table 1
Main facts and features of the Eiffel tower.

Contractor	Gustave Eiffel	First floor	
Engineers	Maurcie Koechlin, Emile Nouguier	Height of the platform	58 m
Architect	Stephen Sauvestre	Length of sides	71 m
Construction	28 January 1887–31 March 1889	Intermediate floor	
Composition	18,000 metal components. 2,500,000 rivets	Height of the platform	116 m
Total weight (according to the original drawings)	10,100 tons (7300 tons of the metal structure)	Length of sides	41 m
Total weight (at present)	11,700 tons	Third floor	
Length of each side of the tower at ground level	125 m	Height of the platform	312 m (in 1889) 324 m (today)
Gap between the feet	72 m	Length of sides	18.6 m
Width of feet	26 m		

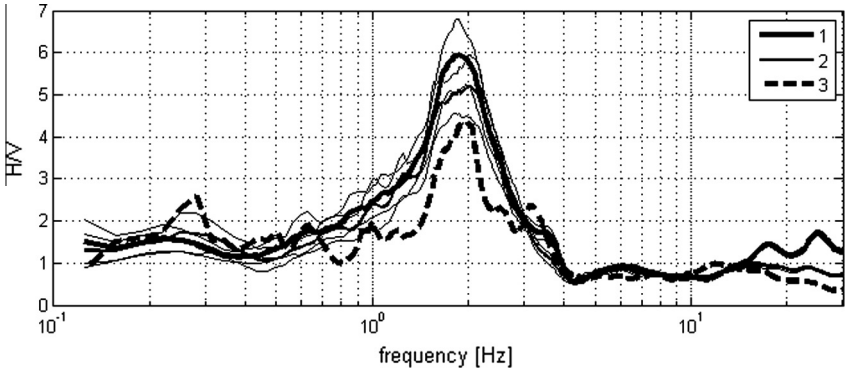

Fig. 2. H/V curves (average ± standard deviation) acquired on the ground at the locations indicated in Fig. 1. A 2 Hz resonance frequency is clearly visible at all sites and is interpreted as the resonance of about 50 m sediments overlying the local bedrock.

functions and the standard deviations were then calculated and are illustrated in Fig. 2, where a dominant resonance frequency at 2 Hz is clearly visible at all sites.

A multichannel analysis of surface waves ([23]) acquired in 2014 at a nearby site for a construction engineering work, was kindly provided by the company Miage (Laval, France, Fig. 3B) and the joint fit of the H/V and dispersion curves allowed us to get a V_S (and therefore a stiffness) profile of the foundation subsoil of the Eiffel tower down to approximately 50 m, where the bedrock responsible for the 2 Hz resonance is located. The theoretical H/V and dispersion curves were obtained though the Grilla software written by one of the author (S.C.) and described in Castellaro and Mulargia [5].

2.2. The tower

The location, number and duration of the measurements inside the tower was conditioned by the accessibility (the centre of each platform, for example, is not accessible with the sole exception of level 2). The same portable seismometer used for the survey on the ground ($10 \times 7 \times 14$ cm, <1 kg) was then placed inside a paper shopping bag (Fig. 4) in order not to distract other visitors (whose transit close to the instrument would disturb the measurements) and we kept it stored inside the shopping bag during all the recordings.

We recorded ambient vibrations at the 3 platforms (55 m, 116, 270 m height), along the south pillar, as shown in Fig. 5. At all levels we took two 10 min (1024 samples per second) recordings, one with the instrument horizontal axis parallel to the tower rim and the other with the instrument horizontal axis set along the diagonals of the tower. The two sets of measurements are in some way redundant, since they just measure the same motion in two different coordinate systems. However, we took two recordings at each level and at close distance for cross-check. On the second floor we managed to take an additional recording approximately in the centre of the platform, where the toilets are presently located. We used this recording to better recognize the torsion modes.

The observation of the spectral peak frequencies (Figs. 6–8) allows us to identify the main vibration modes of the tower and the observation of the spectral inter-plane and intra-plane amplitudes allows us to make precise inferences about the mode shapes (see the discussion for more information about the requirement of stationarity of the excitation function). We note that since we used a seismometer for the recordings, the output data are in velocity (here we use mm/s). In Fig. 9, however, we show the module (i.e. the absolute value) of the recorded mode shapes in displacement.

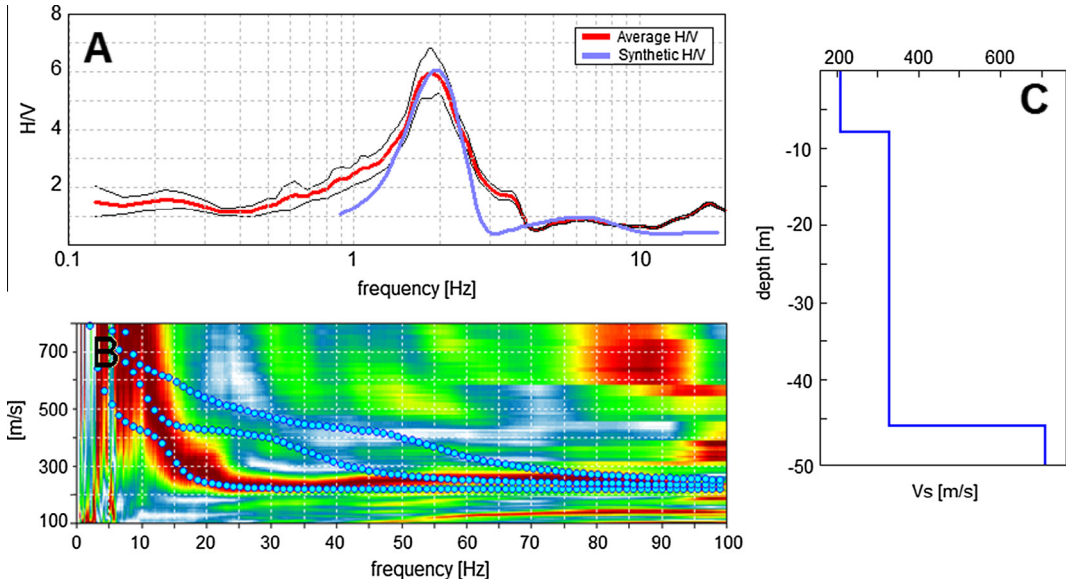

Fig. 3. Joint fit of the H/V (panel A) and MASW (panel B) recordings to get a Vs profile of the subsoil (panel C).

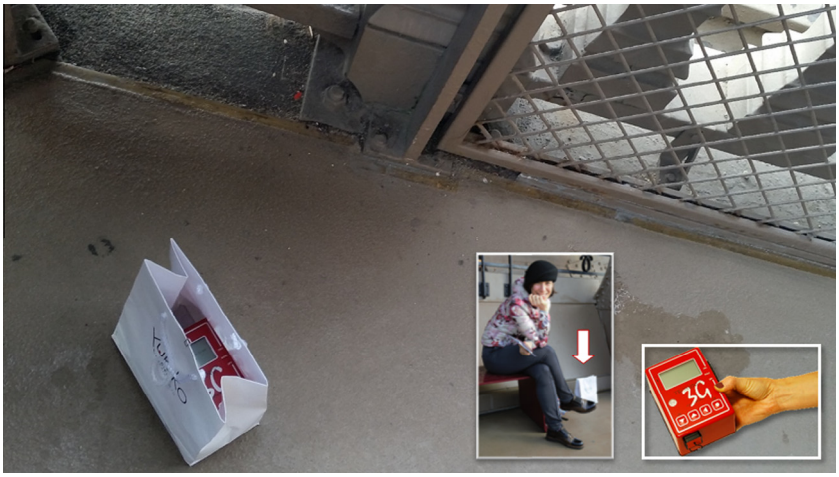

Fig. 4. The pocket seismometer (Tromino®) used in this study during a recording on the first level of the Eiffel tower. The frames on the right illustrate the size of the device and the way we took the recordings. The instrument was placed inside a paper shopping bag to prevent visitors from getting close to it to ask questions. People transit too close to the instrument would affect its measurements. We sat/stood next to the bag for the whole duration of the recordings.

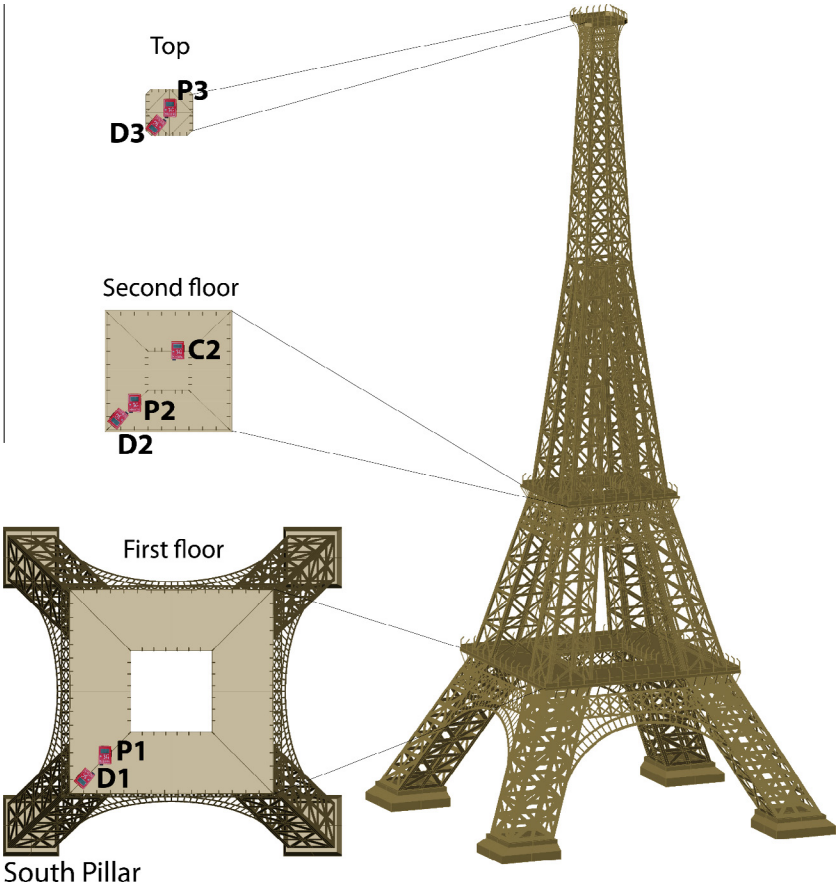

Fig. 5. Location of the measurement inside the tower and instrumental orientation. P stands for parallel (to the tower rim), D stands for diagonal, C for central. The number refers to the level.

We get the module of the mode shape and not the real mode shape because our recordings were not synchronous at the different levels and we could not derive information on the phase of the signal among the different levels. However, this makes a difference only for modes higher than the fundamental one and getting the absolute value of the mode shape is still an important information in the mode identification.

The first horizontal flexion mode of the tower appears clearly at the frequency of 0.32 Hz (period of 3.1 s, Fig. 6). At this frequency the motion involves particularly the upper part of the tower, however a large vertical rocking is also observed at all levels, which implies that the ground participates to this movement and that the soil-structure interaction cannot be neglected in the models [32,33].

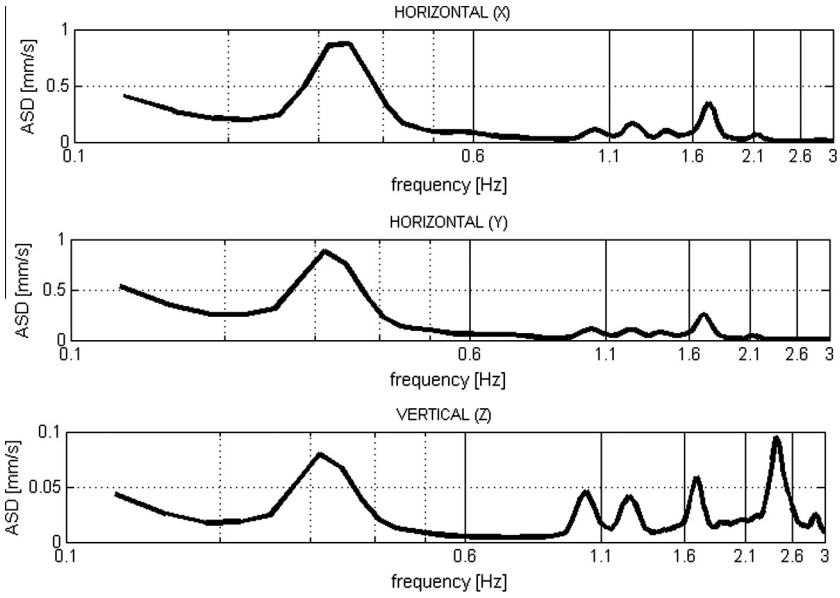

Fig. 6. First flexion/rocking mode of the tower (0.32 Hz) as measured at the top level. Note that the vertical scale is one order of magnitude smaller than the horizontal ones. ASD stands for Amplitude Spectral Density.

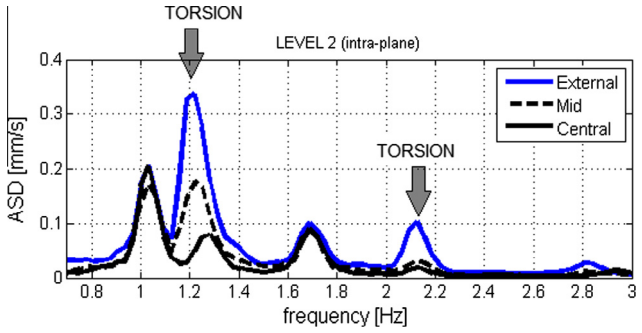

Fig. 7. Horizontal spectra recorded at the second level of the tower in external, intermediate and central positions (D2, P2, C2 in Fig. 5). Torsion modes can be easily recognized because the linear velocity at the centre of the level must be much lower compared to the peripheral positions: this occurs at 1.3 and 2.1 Hz. Flexion modes, on the opposite, displace the same floor with the same amplitude: this occurs at 1 and 1.7 Hz. The mode sequence in this picture is therefore flexion (1 Hz), torsion (1.3 Hz), flexion (1.7 Hz) and torsion (2.1 Hz). ASD stands for Amplitude Spectral Density.

A second horizontal flexion mode appears at 1 Hz (1 s) and can be classified as a flexion because the linear velocity of motion of the central and peripheral locations is the same (Fig. 7).

A third mode appears at 1.2 Hz (0.8 s), which must be a torsion because the linear velocity of motion in the centre tends to zero compared to the peripheral locations (Fig. 7).

Then again we have two horizontal flexion modes (1.4 and 1.7 Hz) and a second torsion mode (2.1 Hz, Figs. 7 and 8). The experimental findings are summarized in Table 2.

The absolute horizontal displacements recorded at each level and for each mode are illustrated in Fig. 9. The mass distribution is definitely not linear along the tower. From the original drawings in Eiffel [10] we have estimated that 5,920,000 kg can be referred to the measurements on the first floor, 2,485,000 kg can be traced back to the motion recorded on the second floor and 1,272,000 kg to the motion recorded on the third floor. We will therefore compute the percentage of the mass participating to each modal movement by attributing 61%, 26% and 13% of the total mass to the first, second and third floor displacement respectively. As shown in Table 2, this suggests that the fraction of the total mass moved in the horizontal component at mode 1 is 40%, followed by 5 modes with approximately the same importance (they move 5–7% of the total mass each).

3. Finite element model (FEM)

We constructed a geometrical model of the tower (Fig. 5), faithfully reproducing the original drawing by Eiffel [10]. From these we derived both the structural and non-structural masses. Some of the latter were removed from the model because they do not exist anymore (e.g. some machineries installed between the second and the third floor that served for the elevators) while other non-structural masses were added because they did not exist in the original drawings (e.g., the radio antennas on the top and other devices). Details in the following discussion.

From the geometrical model, we built a 3-dimensional finite element model with the software MIDAS GEN rel. 8.4.0 (MIDAS-FEA), consisting in 3472 nodes and 8773 elements. The non-structural masses have been applied to 1143 nodes. The beams have been divided only at the nodes connecting them with other beams, in order to avoid local vibration modes, not interesting in this study. The floors were modelled as stiff layers.

We used BEAM elements (6 degree of freedom end nodes grouped into 57 different sections, see Appendices A and B), in place of the more common TRUSS elements [29], characterized by normal stress only, because some beams (e.g. the face diagonals) have a complex lattice structure with high flexion stiffness.

The elements, which were built with puddled iron (i.e. low carbon content iron) were modelled as S355 according to the modern classification systems (European Norm 10,025).

As stated in the previous section, the strong rocking observed (which implies a ground deformation), suggested to model the soil-structure interaction. To this aim we connected the 4 foundations of each leg to the ground through 3-axial Winkler springs, characterized by vertical stiffness $k = 3\ kg/cm^3$, applied to each of the 16 foundation elements (6×15 m each). However, we observed that the Winkler module (whatever its value) does not affect the model result to a significant extent, probably because the vertical stress is only $0.8\ kg/cm^2$ (11,700 tons divided by

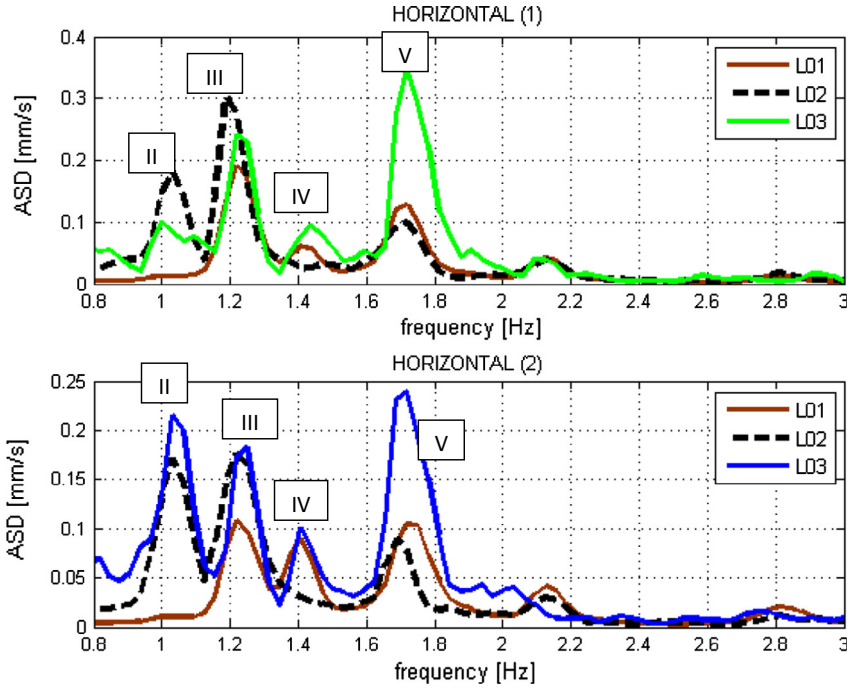

Fig. 8. Horizontal spectra recorded at the 3 levels in the two horizontal directions parallel to the tower rim in the frequency interval [0.8, 3] Hz, which means that the first flexion mode is external to the figure (this can be seen in Fig. 6). ASD stands for Amplitude Spectral Density.

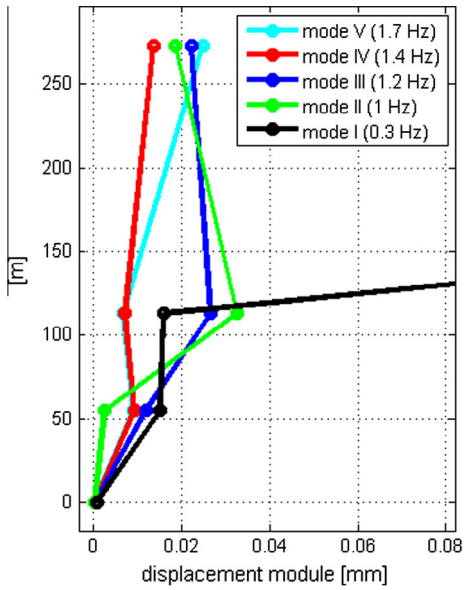

Fig. 9. Modules of the maximum horizontal displacement recorded at the different levels of the tower at the first 5 modal frequencies. The amplitude of the first flexion mode is much larger at the top level than the others (0.56 mm), so that it goes out of the image.

$16 \times 6 \times 15$ m^2), which can be supported by even poor quality subsoils at 7 m depth. More in detail, by changing the Winkler module of a factor 10^2 (from 0.3 to 30 kg/cm^3) we observed a shift of the first mode just from 0.33 to 0.35 Hz, of the second mode from 1.07 to 1.21 Hz and of the third model from 1.18 to 1.32 Hz. Therefore, we can state that to the aim of the present analysis, the Winkler module has not a first order effect.

The model was tuned several times in order to match the experimental results. Our first attempt reproduced the original drawings of Eiffel (10,100 tons), with a dead load at the third level of 60 tons and the first flexion mode that we got from this model was located at 0.45 Hz.

The actual presence of the telecommunication installations on the top of the tower suggested a first increase of the mass on the top up to 250 tons, so that the first flexion mode frequency shifted to 0.37 Hz, while upper modes remained substantially unaffected.

However, according to the article printed in Le Moniteur [21], the present mass of the tower is 11,700 tons. Since the structural elements have not changed since 1989, the extra mass has to be referred to dead loads at the different levels. We therefore distributed this dead load according to the surface of the levels, and also considering that the first floor is actually composed of 2 platforms. At the end, we increased the dead load at the first level of 800 tons, at the second level of 400 tons and at the top level of 360 tons. In this way we managed to reproduce the experimental modal frequencies, as described in Table 3 and illustrated in Fig. 10.

4. Resistance to horizontal actions

4.1. Seismic actions

According to the most recent European Seismic Hazard Map (SHARE Consortium, [39]) the bedrock Peak Ground Acceleration (PGA_0) with 10% exceedance probability in 50 years in Paris is equal to 0.02 g (return period 475 years) while the PGA_0 with 2% exceedance probability (return period 2475 years) is lower than 0.05 g. In order to verify the seismic vulnerability of the Eiffel tower, we selected 15 accelerometric recordings of real earthquakes characterized by $PGA_0 = [0.05, 0.1]$ g and occurred on stiff subsoils by using the ITACA [18] database (Fig. 11). We extended the PGA_0 range compared to the assumptions stated above in order to account for the uncertainty intrinsic in the seismic hazard assessment estimates. Then, we computed the bedrock-to-surface transfer function by using the subsoil model discussed in Section 2.1. Our reference surface is the foundation level of the tower, 7 m below the actual ground level. By using the 15 selected input

Table 2
Summary of the main modal frequencies of the Eiffel tower.

No.	Frequency [Hz]	Period [s]	Mode name/ mechanism	% of mass (horizontal only)	Justification
1	0.32	3.1	Horizontal flexion (I)	40	At this frequency the motion involves mostly the upper-thin part of the tower. A vertical motion (rocking) is observed at all levels and this implies a deformation of the ground and the fact that the soil-structure interaction cannot be neglected
2	1	1	Horizontal flexion (II)	7	Same linear velocity in the central and peripheral location. It is invisible at level 2
3	1.2	0.8	Torsion (I)	7	Lower linear velocity in the centre compared to the periphery, which is clearly visible at level 2
4	1.4	0.7	Horizontal flexion (III)	5	Same linear velocity in the central and peripheral location. It is invisible at level 2
5	1.7	0.59	Horizontal flexion (IV)	6	Same linear velocity in the central and peripheral location
6	2.1	0.48	Torsion (II)		Lower linear velocity in the centre compared to the periphery

Table 3
Comparison of the experimental and the modelled modal frequencies and mechanisms of the Eiffel tower.

	Experimental		Modelled	
No.	Frequency [Hz]	Mode name/mechanism	Frequency [Hz]	Mode name/mechanism
1	0.32	Horizontal flexion (I)	0.33	Flexion
2	1	Horizontal flexion (II)	1.07	Flexion
3	1.2	Torsion (I)	1.18	Torsion
4	1.4	Horizontal flexion (III)	1.25	Flexion
5	1.7	Horizontal flexion (IV)	1.62	Torsion
6	2.1	Torsion (II)	1.8	Torsion
7			2.2	Torsion

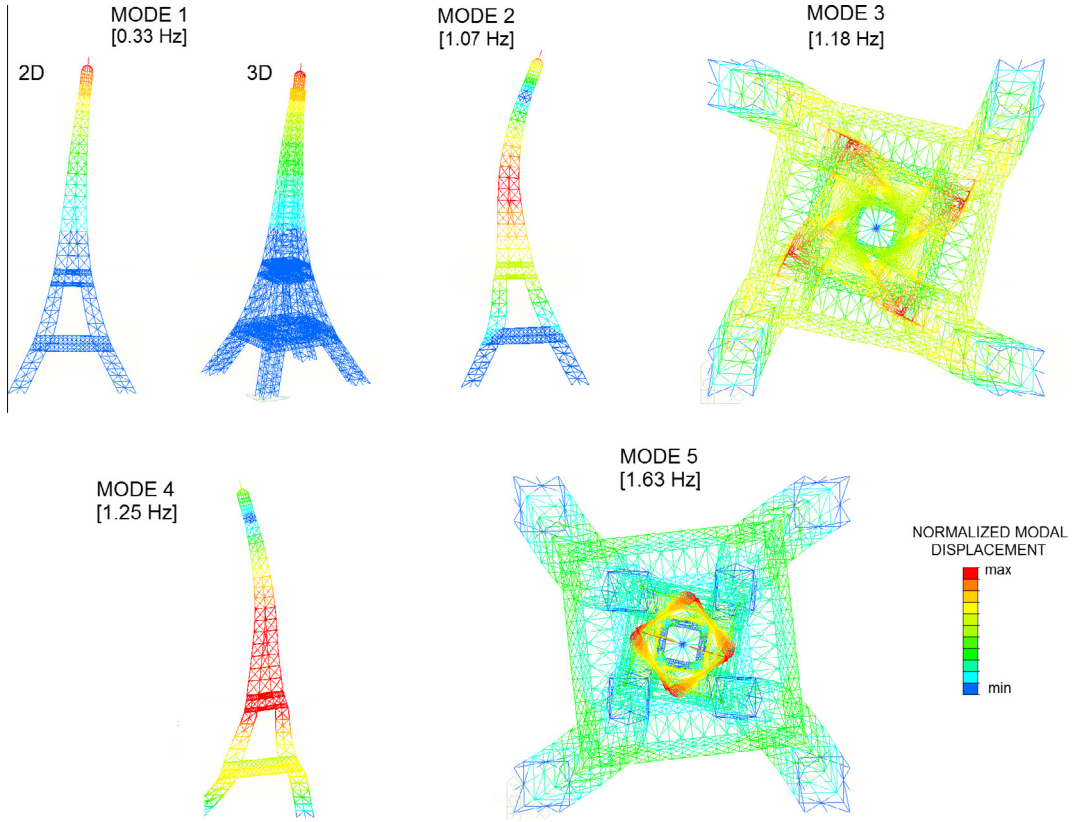

Fig. 10. Mode shapes of the first 5 modes of the Eiffel tower from the FEM. Torsion modes (3 and 5) are shown in the horizontal plane. Flexion modes (1, 2, 4) are shown in the vertical plane.

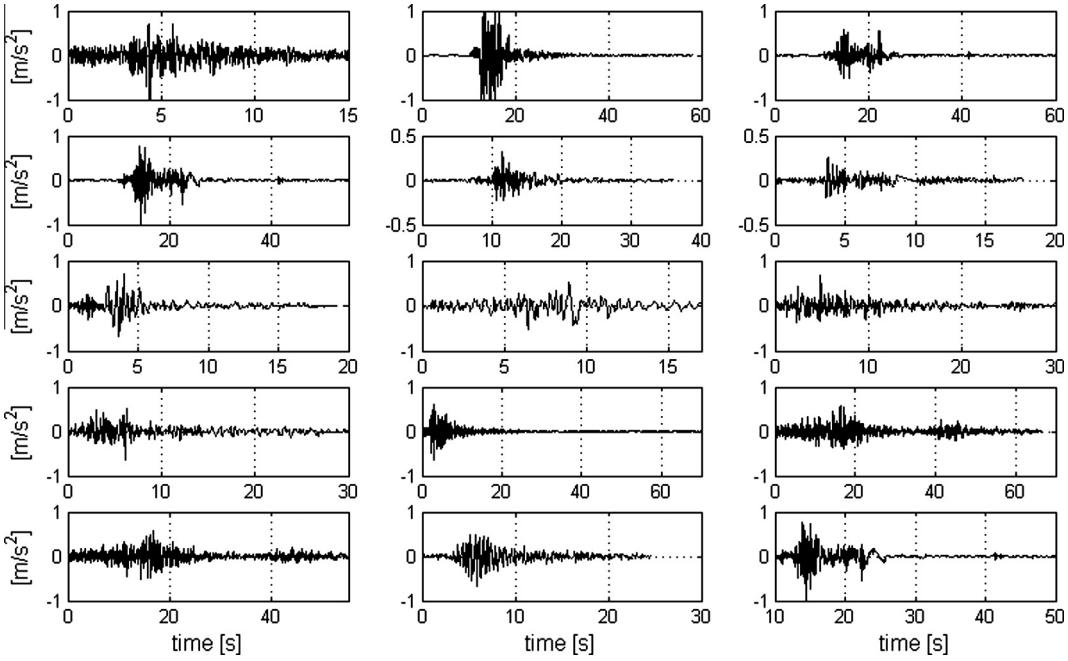

Fig. 11. The 15 real ground motions (accelerations) with PGA_0 = [0.05, 0.1]g (referring to the stiff bedrock conditions) selected for the seismic response analysis.

motions on the bedrock and the computed bedrock-to-surface transfer functions, we calculated the response spectra of the tower (mean ± standard deviation in red in Fig. 12). To this aim we used the 1D equivalent-linear code EERA by Bardet et al. [1] Appendix C. The PGA expected on the foundation level of the Eiffel tower can be read at period T = 0 s in the response spectra (Fig. 12) and is on average 0.15 g. The spectral acceleration at 0.3 Hz (the first flexion mode of the tower) is on average 0.02 g.

We computed the stress on the main tower beams induced by the dead load, which has a maximum value of approximately 80 MPa at the bottom of the tower (Fig. 13A). Then, we used the mean + standard deviation response spectrum (upper red dashed curve in Fig. 12) as input of our FE model to calculate what PGA could bring the tower to yielding. We see (Fig. 13B) that the maximum stress induced on the tower from the considered earthquakes is approximately 50 MPa and occurs close to the first level of the tower, not on the same beams subjected to the maximum dead load.

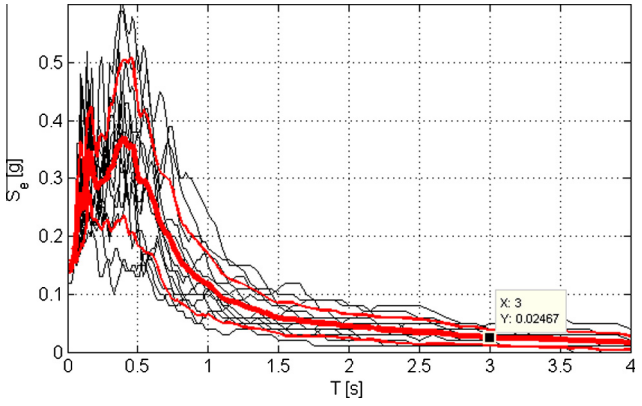

Fig. 12. Response spectra computed for each input ground motion of Fig. 11 after its convolution with the site response function (black lines). Mean values and standard deviations in red. (For interpretation of the references to colour in this figure legend, the reader is referred to the web version of this article.)

We do not know the exact mechanical parameters of the puddled iron used in the tower. Therefore, we consider average values published in the literature for this kind of material [22] which are approximately [220,370] MPa for the ultimate tensile and compression strength and [160,220] MPa for the yield point. By observing that the dead loads are fixed loads, it follows that we can accept an earthquake induced PGA > 100% larger than the expected values [0.05, 0.1]g before the tower reaches the yielding stress.

4.2. Wind

Eiffel ([10], see also the translation in [25]) studied the stress of the tower under two wind configurations. At that time, he could only approach the problem from a static planar point of view, following the Culmann graphic method [8]. At present, detailed wind numerical analyses are possible but this is not the aim of the present paper. Here we approach the study of the wind induced displacements with a 3D FE static approach, with the only purpose of validating our model with Eiffel's calculations.

The first wind action studied by Eiffel consisted in a uniform load of 3 kN/m^2 on the whole height. The second configuration consisted in a linearly increasing load with height, ranging from 2 to 4 kN/m^2. These apparently high values correspond to the modern evaluation of the pressure coefficient of lattice structures. First, we verified that the forces computed with our FE model in the beams at the different levels corresponded to those reported in the Eiffel original project ([10], Fig. 7) and we found that the differences were acceptable (maximum 12%), particularly considering that the 3D FE modelling provides less discretized values compared to what was possible at Eiffel's time. An example of this comparison is reported in Table 4 and refers to the section XXVII plate XXXII (Fig. 7) in Eiffel [10].

After this check, we found that for the uniform wind configuration (3 kN/m^2) the maximum displacement clearly occurs on the top of the tower and is around 60 cm, while for the variable (2–4 kN/m^2) wind configuration the maximum displacement is 70 cm, always on the top of the tower (Fig. 14).

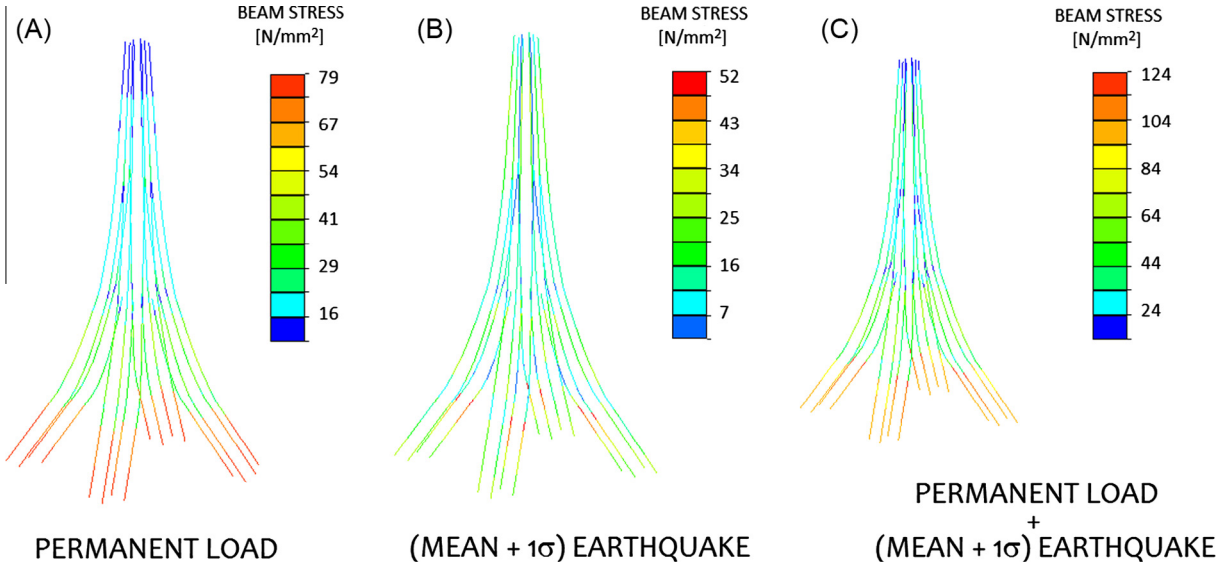

Fig. 13. (A) Values (in MPa) of the dead stress on the main beams; (B) of the stresses induced on the beams from the average + 1 standard deviation earthquake expected at the site with a 2% probability of being exceeded in 50 years (centre); and (C) sum of the stresses in (A) and (B).

Table 4
Forces in the beams (for each leg) as computed by Eiffel [10] due to the dead load and to two wind configurations, compared with the results from the FE model. Differences are in the order of 12% in all cases.

	Maximum forces in the beams (for single leg)	
	Due to uniform wind (3 kN/m^2)	Due to dead load
Eiffel's calculations	9827.5 kN	20,775 kN
FEM	11,670 ± 60 kN	26,850 ± 60 kN
	Variable wind (2–4 kN/m^2)	
Eiffel's calculations	9579.5 kN	
FEM	11,450 ± 10 kN	

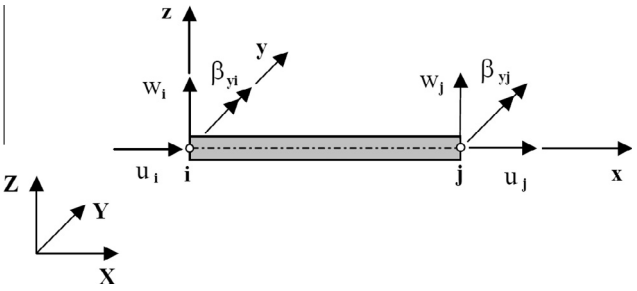

Fig. 15. A 2D prismatic beam element.

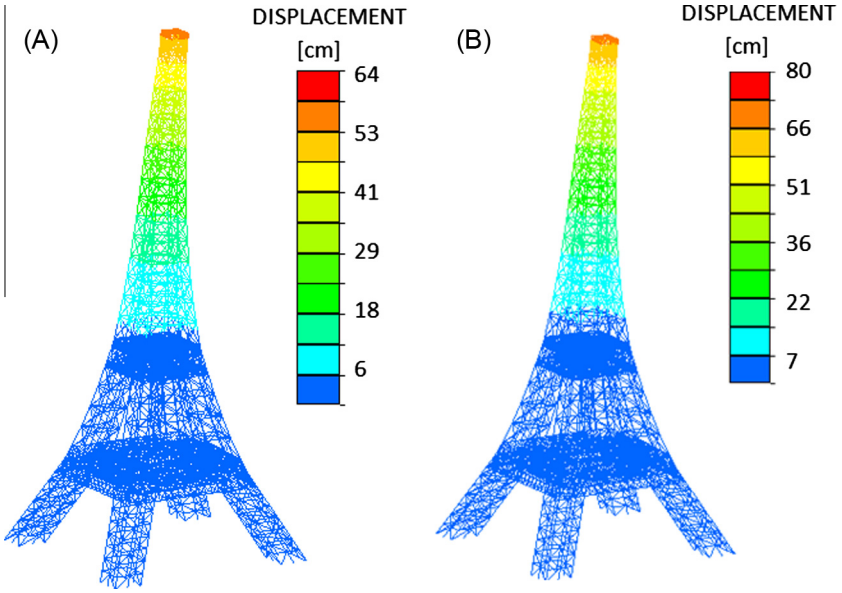

Fig. 14. Displacement (in cm) of the tower (A) for a uniform wind load of 3 kN/m^2 and (B) for a linearly increasing wind load from 2 to 4 kN/m^2.

According to Roland and Weidman [25], who translated Eiffel's technical drawing, the computed displacement would be 22 cm for a pressure of 78 kg/m^2, which is in line with our findings.

5. Discussion and conclusions

The Eiffel tower is the most visited and popular monument in the world. It is also a unique structure. While there exist hundreds of architectural drawings of the tower, we could not find any dynamic characterization of its behavior.

In this paper we show that such an important structure can be sufficiently characterized in a fully passive, fast and cheap way, under operative conditions. We achieved this goal by taking basically 4 measurements (1 per level at the external rim plus a central one) of 6–10′ min, that is in less than one-hour work.

The modal frequencies of the tower appear as clear peaks in the spectra of the recorded motion. The observation of the peak amplitudes allowed us to reconstruct the mode shapes and the percentage of the total mass moved by each mode. We must recall that while the mode frequencies are correctly identified even with a single instrument moved at different locations, the mode shapes are correctly reconstructed – in the passive analysis – only under the hypothesis of stationary vibration source. If this requirement does not hold, then a reference instrument is needed. The main vibration sources at frequencies below 2 Hz in nature are the atmospheric perturbations [15,16,17,31,36]: during the survey, which lasted less than 2 h, the weather and wind conditions remained stable. On that November morning there were also very few tourists on the tower and care was taken in removing transients due to the movement of people from the spectra analysis. Therefore, we believe that the amplitude of the spectra recorded at the different level in different (but close) times, still reflects the mode shapes to a good extent.

However, we note that working with a single instrument the phase information, that is needed to reconstruct the mode shapes beyond the first flexion mode (characterized by displacements with the same sign at any level), is not available [30,13]. What we got is therefore the absolute value of the mode shape, which is nonetheless informative.

We found that the first flexion mode, which moves approximately the 40% of the tower mass in the horizontal plane, has a frequency of 0.32 Hz. The displacement on the top of the tower due to this motion is almost 2 orders of magnitude larger than on the second floor. Large rocking (which shows up as a large amplification of the vertical spectra at this frequency) is observed at all levels and implies the ground participation to the tower movement. The soil-structure interaction should therefore not be disregarded in the model.

The following 5 modes (flexion, torsion, flexion, flexion, torsion) move 5–7% of the mass each in the horizontal plane.

We also explored the subsoil around the tower. According to the drillings of the late 1800, more than 15 m of alluvial sediments (sands and silts) are present under the tower. We actually measured a clear resonance frequency at 2 Hz that, modelled jointly with a surface wave dispersion curve available at a nearby site, stands for the local bedrock at approximately 50 m depth and for an average shear wave velocity of 250 m/s in the shallow alluvial layers.

Assessing the resonance frequencies of structures and soil is important in seismic countries to identify conditions of double resonance (e.g., [6]). In this case the subsoil resonance frequency coincides with the frequency of the 6th mode, which is a torsion. However, seismic hazard in Paris is low and the dynamic characterization of the tower is not of primary interest in this respect. However, by using the finite elements model of the tower and the bedrock-to-surface transfer function reconstructed from the measurements on the subsoil, we studied the response of the tower to the characteristic earthquakes expected in Paris with a return period of 475 and 2475 years, respectively (that is to peak ground accelerations on the bedrock in the range [0.05, 0.1]g). We found that the tower could undergo PGA values >100% larger than those expected from the seismic hazard maps before reaching the yielding stress. The modal analysis of the tower is relevant for several other reasons: first, to the wind actions. Gustave Eiffel studied the effect of wind on the tower but he could only approach this from a static planar point of view [10]. We studied the displacements under the same extreme wind configurations studied by Eiffel, by using the 3D FE model tuned on the experimental data. We found that for a uniform wind load of 3 kN/m^2, the maximum displacement can be as large as 60 cm, while for a linearly increasing wind load, from 2 to 4 kN/m^2 the maximum displacement can be in the order of 70 cm. This analysis was performed in order to verify our model, within a 3D scheme, against the Eiffel's calculation and is not meant to be a dynamic modern wind analysis.

The modal analysis of the tower turns out to be interesting also because the tower is very tall and light, which means that it is an unusual structure with a large stiffness and a small mass, whose behavior escapes intuitive forecasts.

Last, we think that it is quite impressive what can nowadays be done in terms of structural characterization with a few minutes of recordings on a structure, with no need for bulky equipment, induced excitations, sophisticated software. Our 1-h work on the tower is certainly not the most accurate survey than could be planned on such a structure but it shows to be enough to characterize the first 6 modes of the tower, that is what really matters in the standard engineering practice.

Millions of visitors have taken millions of pictures of the Eiffel tower over the last century. What we did in this work is a different kind of photography (better saying video) of the tower, which fixes the dynamic behavior of the tower at present. As many times in the past, the non-structural masses of the tower are going to change several more times in the future with the replacement of the elevators and of the antennas on the top, with different shops at the lower levels, etc. The knowledge of the dynamic response of the tower is important in the engineering practice to better design the future interventions and to monitor the ageing of the structure.

In the end, this paper also wants to be a tribute to the people whose freedom was caught by a terroristic attack the same day (November 13th, 2015) in which we got the freedom to take a plane to Pairs with a seismometer in the backpack to see who of us won the bet of getting the first mode frequency of the tower right.

Acknowledgments

We thank Miage (France) for providing the MASW recording.

Appendix A

The beam element incorporated in the FE code (MIDAS, further details in http://en.midasuser.com/, last accessed August 2016) used in this paper is a three-dimensional beam, under the following assumptions:

- The element is a straight bar of uniform cross-section,
- The beam cross-section is a closed solid (thick-walled) section,
- The element cross-section bending and shear centers are coincident,

- The element is capable of resisting axial forces, bending moments along the two main axes in the plane of its cross-section, and twisting moments in respect to its centroid axis,
- The transverse shear effects are modelled according to the Timoshenko beam theory,
- Torsional behavior is governed by the Poisson's theory of torsion (warping is not allowed),
- The element ends can be hinges,
- The element ends can be end-offsets along the local axes.

For convenience, we reduce the formulation of the prismatic, isotropic beam element for the effects of transverse shear deformation to the 2D case, as in Fig. 15. According to the Timoshenko beam theory, the plane normal to the neutral axis remains plane after deformation. However, this plane is no longer normal to the neutral axis due to the shear deformation. The total rotation of the plane normal to the unstrained neutral axis is the sum of the rotation of the tangential line to the neutral axis and the rotation due to shear deformation:

$$\beta = -\frac{\partial w}{\partial x} + \gamma$$

where γ is the shear strain, constant over the cross-section. Since the shear stress and strain vary over the cross-section, the shear strain γ is an equivalent constant strain corresponding to the shear area:

$$\tau = \frac{V}{A_s}; \quad \gamma = \frac{\tau}{G}$$

where V is the shear force at the considered cross-section.

On the basis of these assumptions, the finite element formulation is obtained by the fundamental virtual work principle or the principle of total minimum potential energy, which is expressed as follows for the beam of Fig. 15.

$$\Pi = \frac{EI}{2}\int_0^L \frac{\partial \beta}{\partial x}dx + \frac{GA_S}{2}\int_0^L \left(\frac{\partial w}{\partial x} - \beta\right)^2 dx + \int_0^L pwdx - \int_0^L m\beta dx$$

where p and m represent the lateral force and moment per length unit, respectively. The first two terms on the right side of the equation represent the strain energy corresponding to the flexure and shear deformations. The last two integration terms represent the potential energy of the external forces. The condition for the minimum potential energy $\delta\Pi = 0$ is the basis for the formulation of a beam element with shear deformation.

Appendix B

Properties of the 57 types of BEAM elements used in the FE model of the Eiffel tower.

ID	Type	Shape	Name	Area_x [cm^2]	Area_y [cm^2]	Area_z [cm^2]	Ixx [cm^4]	Iyy [cm^4]	Izz [cm^4]
1	Value	B	Section XXVIII	909	472	472	1,349,400	900,917	900,917
2	Value	B	Section XXVII	880	456	456	1,308,740	873,683	873,683
3	Value	B	Section XXVI	865	448	448	1,288,280	859,982	859,982
4	Value	B	Section XXV	835	432	432	1,247,100	832,416	832,416
5	Value	B	Section XXIV	775	400	400	1,163,710	776,615	776,615
6	Value	B	Section XXIII	670	344	344	1,014,410	676,790	676,790
7	Value	B	Section XXII	654	336	336	992,731	662,302	662,302
8	Value	B	Section XXI	578	296	296	882,996	588,994	588,994
9	Value	B	Section XX	548	280	280	838,477	559,264	559,264
10	Value	B	Section XIX	548	280	280	838,477	559,264	559,264
11	Value	B	Section XVIII	548	280	280	838,477	559,264	559,264
12	Value	B	Section XVII_s	651	350	350	351,906	235,933	235,933
13	Value	B	Section XVI_s	651	350	350	351,906	235,933	235,933
14	Value	B	Section XV_s	651	350	350	351,906	235,933	235,933
15	Value	B	Section XIV_s	651	350	350	351,906	235,933	235,933
16	Value	B	Section XIII_s	651	350	350	351,906	235,933	235,933
17	Value	B	Section XII_s	651	350	350	351,906	235,933	235,933
18	Value	B	Section XI_s	668	360	360	359,630	241,197	241,197
19	Value	L	Section X_s	564	250	250	6768	131,258	131,258
20	Value	L	Section IX_s	538	238	238	5821	125,746	125,746
21	Value	L	Section VIII_s	538	238	238	5821	125,746	125,746
22	Value	L	Section VII_s	384	167	167	2048	92,608	92,608
23	Value	L	Section VI_s	384	167	167	2048	92,608	92,608
24	Value	L	Section V_s	384	167	167	2048	92,608	92,608
25	Value	L	Section IV_s	384	167	167	2048	92,608	92,608
26	Value	L	Section III_s	384	167	167	2048	92,608	92,608
27	Value	L	Section II_s	384	167	167	2048	92,608	92,608
28	Value	L	Section I_s	319	138	138	1158	77,961	77,961
29	Value	B	Section XVII_c	412	215	215	235,551	157,351	157,351
30	Value	B	Section XVI_c	412	215	215	235,551	157,351	157,351
31	Value	B	Section XV_c	412	215	215	235,551	157,351	157,351
32	Value	B	Section XIV_c	366	190	190	211,441	141,180	141,180
33	Value	B	Section XIII_c	263	135	135	155,447	103,711	103,711

Appendix B (*continued*)

ID	Type	Shape	Name	Area_x [cm^2]	Area_y [cm^2]	Area_z [cm^2]	Ixx [cm^4]	Iyy [cm^4]	Izz [cm^4]
34	Value	B	Section XII_c	263	135	135	155,447	103,711	103,711
35	Combined	2T1	Section XI_c	157	112	25	191	55,148	23,717
36	Combined	2T1	Section X_c	204	142	38	355	82,839	28,419
37	Combined	2T1	Section IX_c	204	142	38	355	82,839	28,419
38	Combined	2T1	Section VIII_c	204	142	38	355	82,839	28,419
39	Combined	2T1	Section VII_c	204	142	38	355	82,839	28,419
40	Combined	2T1	Section VI_c	204	142	38	355	82,839	28,419
41	Combined	2T1	Section V_c	204	142	38	355	82,839	28,419
42	Combined	2T1	Section IV_c	204	142	38	355	82,839	28,419
43	Combined	2T1	Section III_c	204	142	38	355	82,839	28,419
44	Combined	2T1	Section II_c	204	142	38	355	82,839	28,419
45	Combined	2T1	Section I_c	204	142	38	355	82,839	28,419
46	Combined	2T1	Top elements	204	142	38	355	82,839	28,419
47	DB/User	2L	Horiz. Diagonals II–III level	24	11	11	5	147	25,512
48	Combined	4L	4L80x8 VERT	49	21	21	10	57,502	57,502
49	Combined	I2T	Horiz. Diagonals 0–II level	178	57	98	47	76,134	384,081
50	Combined	4L	4L45x5	17	8	8	1	23,065	23,065
51	Combined	4L	4L80×8	49	21	21	10	57,502	57,502
52	Combined	4L	4L80×10	60	27	27	20	71,220	71,220
53	DB/User	2L	Horiz. Diagonals I floor	24	11	11	5	147	25,512
54	DB/User	2L	2L70×7	19	8	8	3	86	204
55	DB/User	2L	2L80×8	24	11	11	5	147	337
56	Value	2C	Ist floor beams Diagonal	154	13	144	190	18,526	200,909

Appendix C

During past earthquakes, the ground motion on soft soil sites was found to be larger than on nearby rock outcrops, depending on local soil conditions (e.g., [27]). These amplifications of soil site responses started to be simulated in several ways, usually assuming simplified soil deposit conditions such as horizontal soil layers of infinite extent subjected to transient and vertically travelling shear waves. The classical approach assumes that the cyclic soil behavior can be simulated using an equivalent linear model, which is extensively described in the geotechnical earthquake engineering literature (e.g., [27,20]). The wave propagation solutions used are those of Kanai [19], Roesset and Whitman [24], and Tsai and Housner [34]. The equivalent linear model represents the soil stress-strain response based on a Kelvin-Voigt (spring-mass-damper) model. For some of the limits of these models see also Castellaro and Mulargia [7].

References

[1] Bardet JP, Ichii K, Lin H. Equivalent-linear earthquake site response analyses of layered soil, computer program; 2000.
[2] Briaud JL. Geotechnical engineering: unsaturated and saturated soils. John Wiley & Sons; 2013. p. 1024.
[3] BRGM. Cartes géologiques harmonisées à 1/50000. Bureay de Recherches Géologiques et Minières, Service Géologique National Français; 2015. Available from: http:// infoterre.brgm.fr/.
[4] Castellaro S. The complementarity of H/V and dispersion curves. Geophysics 2016 [in press].
[5] Castellaro S, Mulargia F. Constrained H/V only estimates of Vs30. Bull Seism Soc Am 2009;99:761–73. http://dx.doi.org/10.1785/0120080179.
[6] Castellaro S, Mulargia F, Padron Hernandez LA. The different response of apparently identical structures: a far-filed lesson from the Mirandola 20th May 2012 earthquake. Bull Earthq Eng 2013;12:2481–93.
[7] Castellaro S, Mulargia F. Simplified seismic soil classification: the VfZ matrix. Bull Earthq Eng 2014;12:735–54. http://dx.doi.org/10.1007/s10518-013-9543-3.
[8] Culman K., 1865. Die graphische Statik (Graphic Statics), Meyer & Zeller ed.
[9] Davenport AG. Past, present and future of wind engineering. J Wind Eng Ind Aerodyn 2002;90:1371–80.
[10] Eiffel G. Tour de 300 m, Société des Imprimeries Lemercier, 57, rue de Seine, Paris, 47 plates. In: Lemoine B., 2015. Taschen: The Eiffel Tower; 1900. 160 pp.
[11] Fäh D, Kind F, Giardini D. A theoretical investigation of average H/V ratios. Geophys J Int 2001;145:535–49.
[12] Gallant J. The shape of the Eiffel Tower. Am J Phys 2002;70:160.
[13] Gallipoli MR, Mucciarelli M, Vona M. Empirical estimate of fundamental frequencies and damping for Italian buildings. Earthq Eng Struct Dyn 2009;38:973–88.
[14] GSHAP. Compilation of the GSHAP regional seismic hazard for Europe. In: Grünthal G, Bosse C, Sellami S, Mayer-Rosa D, Giardini D, editors. Africa and the Middle East. Available from: <http://www.seismo.ethz.ch/static/GSHAP/eu-af-me/euraf.html> [access: January 2016].
[15] Gutenberg B. Microseisms in North America. Bull Seism Soc Am 1931;21:1–24.
[16] Gutenberg B. Microseisms and weather forecasting. Meteorology 1947;4:21–8.
[17] Gutenberg B. Two types of microseisms. J Geophys Res 1958;63:595–7.
[18] ITACA working group. ITalian ACcelerometric Archive, version 2.1; 2016, http://dx.doi.org/10.13127/ITACA/2.1.
[19] Kanai K. Relation between the nature of surface layer and the amplitude of earthquake motions. Bulletin: Tokyo Earthquake Research Institute; 1951.
[20] Kramer SL. Geothecnical Earthquake Engineering. Prentice Hall; 1996. 653 pp.
[21] Le Moniteur. <http://www.lemoniteur.fr/article/la-tour-eiffel-s-offre-sa-version-2-0-12109439>; 2010 [access February 2016].
[22] Oberg E. Machinery's handbook. 29th ed. New York: Industrial Press Inc; 2016. p. 476. ISBN 0-8311-2666-3.
[23] Park CB, Miller RD, Xia J. Multichannel analysis of surface waves. Geophys 1999;64:800–8.
[24] Roesset JM, Whitman RV. Theoretical background for amplification studies, research report no. R69-15, Soils Publications, 231. Cambridge: Massachusetts Institute of Technology; 1969.
[25] Roland C, Weidman P. Proposal for an iron tower: 300 m in height. Archit Res Quart 2004;8:215–45.
[26] Scanlan RWH. Developments in low-speed aeroelasticity in the civil engineering field. AIAA J 1982;20:839–44.
[27] Seed HB, Idriss IM. Soil moduli and damping factors for dynamic response analysis, Report No. UCB/EERC-70/10. Berkeley: Earthquake Engineering Research Center, University of California; 1970 December, 48 p.
[28] SESAME Project. Guidelines for the implementation of the H/V spectral ratio technique on ambient vibrations: measurements, processing and interpretation. SESAME European Research Project WP12, deliverable no. D23.12. <http://sesame-fp5.obs.ujf-grenoble.fr/Papers/HV_User_Guidelines.pdf>; 2004 [accessed 11.05.12].
[29] Smith J, Hodgins J, Oppenheim I, Witkin A. Creating models of truss structures with optimization. ACM Trans Graph 2002;21:295–301.
[30] Snieder R, Safak E. Extracting the building response using seismic interferometry: theory and application to the Millikan Library in Pasadena, California. Bull Seism Soc Am 2006;96:586–98.

[31] Stehly L, Campillo M, Shapiro NM. A study of the seismic noise from its long-range correlation properties. J Geophys Res 2006;111:B10.
[32] Todorovska MI. Seismic interferometry of a soil-structure interaction model with coupled horizontal and rocking response. Bull Seism Soc Am 2009;99:611–25.
[33] Trifunac MD. Review: rotations in structural response. Bull Seism Soc Am 2009;99:626–35.
[34] Tsai NC, Housner GW. Calculation of surface motions of a layered half space. Bull Seismol Soc Am 1970;60:1625–51.
[35] Tuan T, Scherbaum F, Malischewsky PG. On the relationship of peaks and troughs of the ellipticity (*H/V*) of Rayleigh waves and the transmission response of single layer over half-space models. Geophys J Int 2010;184:800–93.
[36] Yang Y, Ritzwoller MH. Characteristics of ambient seismic noise as a source for surface wave tomography. Geochem, Geophys, Geosys 2008;9. http://dx.doi.org/10.1029/2007GC001814.
[37] Weidman PD. Modified shape of the Eiffel Tower determined for an atmospheric boundary-layer wind profile. Phys Fluids 2009;21:067102.
[38] Weidman P, Pinelis I. Model equations for the Eiffel Tower profile: historical perspective and new results. Comptes Rendus Mécanique 2004;332:571–84.
[39] Woessner J, Laurentiu D, Giardini D, Crowley H, Cotton F, Grünthal G, et al. The 2013 European Seismic Hazard Model: key components and results. Bull Earthq Eng 2015;13:3553–96.
[40] Zoeppritz K. Erdbebenwellen VII. VIIb. Über Reflexion und Durchgang seismischer Wellen durch Unstetigkeitsflächen. Nachrichten von der Königlichen Gesellschaft der Wissenschaften zu Göttingen, Mathematisch-physikalische Klasse; 1919. p. 66–84.